

MODEL BIASES IN HIGH-BURNUP FAST REACTOR SIMULATIONS

Nicholas Touran, Jesse Cheatham, and Robert Petroski

TerraPower LLC

TerraPower, LLC. 11235 S.E. 6th St., Suite A-200, Bellevue, WA 98004

ntouran@terrapower.com; jecheatham@terrapower.com; rpetroski@terrapower.com

ABSTRACT

A new code system called the Advanced Reactor Modeling Interface (ARMI) has been developed that loosely couples multiscale, multiphysics nuclear reactor simulations to provide rapid, user-friendly, high-fidelity full systems analysis. Incorporating neutronic, thermal-hydraulic, safety/transient, fuel performance, core mechanical, and economic analyses, ARMI provides “one-click” assessments of many multi-disciplined performance metrics and constraints that historically require iterations between many diverse experts. The capabilities of ARMI are implemented in this study to quantify neutronic biases of various modeling approximations typically made in fast reactor analysis at an equilibrium condition, after many repetitive shuffles. Sensitivities at equilibrium that result in very high discharge burnup are considered (>20% FIMA), as motivated by the development of the Traveling Wave Reactor. Model approximations discussed include homogenization, neutronic and depletion mesh resolution, thermal-hydraulic coupling, explicit control rod insertion, burnup-dependent cross sections, fission product model, burn chain truncation, and dynamic fuel performance. The sensitivities of these approximations on equilibrium discharge burnup, k_{eff} , power density, delayed neutron fraction, and coolant temperature coefficient are discussed.

Key Words: ARMI, TWR, sensitivity, multiphysics, burnup dependence, mesh resolution

1. INTRODUCTION

To support the continuing development of the Traveling Wave Reactor (TWR) and other innovative nuclear reactors, a suite of computational analysis tools have been developed and collected into a common framework as a new code system, the Advanced Reactor Modeling Interface (ARMI). Previous work provided motivations for high-burnup reactors and identified non-traditional constraints that must be considered in their development [1,2]. In this paper, several sources of modeling bias at equilibrium are quantified using ARMI. The study demonstrates the capabilities of ARMI while guiding analysts in understanding the errors associated with common simulation approximations. The burnup dependence of uncertainties due to nuclear data, as discussed elsewhere [3], are not discussed, leaving focus on modeling choices such as homogenization, mesh size, and coupled physics. Parameters studied include reactivity, peak burnup, power density, coolant temperature coefficient, and delayed neutron fraction.

2. SIMULATION TOOLS AND SOFTWARE FRAMEWORK

The Advanced Reactor Modeling Interface (ARMI) is a new code system that performs multiphysics nuclear reactor design calculations by loosely coupling a collection of newly developed and off-the-shelf simulation software. The code accepts highly general and graphical

input to create an object-oriented, composite model of the reactor core, where the reactor is made of assemblies which are in turn made of blocks. State variables (such as power, flux, temperature, burnup, etc.) are stored within the blocks as the simulations proceed. ARMI is platform independent, written primarily as a large Python [4] package, though some of its computationally-intensive kernels are written in hybrid Python/C++.

2.1. General Capabilities of ARMI

ARMI is launched from a simple graphical user interface. From an initial state, ARMI produces inputs for a variety of codes. Primarily, it produces MC²-2 [5] and REBUS-PC [6] inputs to simulate the neutronics. After generating power, flux, and burnup for a cycle, ARMI reads the outputs and adds the values to the in-memory reactor state. Using this new state, it builds inputs and runs a variety of other modular simulations to add additional physics information to the state. Thermal-hydraulic (T/H) codes provide temperatures and pressures, fuel performance codes determine irradiation-induced deformations (and associated fission gas removal, etc.), core mechanical simulations determine duct distortions such as bowing and bulging, and economics modules determine fuel cycle costs. The ARMI safety module produces kinetics parameters and 3-D reactivity coefficients and builds inputs to transient systems codes. Finally, the fuel management module determines how to shuffle fuel using parallelized branch searches. The assemblies are moved within ARMI, and then the calculation loop continues by building new MC²-2 and REBUS-PC inputs and running the second cycle.

The ARMI code stores results in a SQL database as it runs, allowing real-time advanced visualization and post-processing. A custom visualization tool called XTVIEW allows state exploration in time and space. Additionally, the power, flow, temperature, and fluence information from an entire history of assemblies of interest can be automatically composed into inputs for finite-element based fuel performance or duct distortion models. Full lifetime plots of peak cladding temperature (PCT), maximum burnup, maximum fluence, maximum assembly distortion, maximum power density, resources required (feed material and SWUs) and others are automatically generated at the end of each run for rapid assessment of the full performance of any given design iteration.

Any particular ARMI state can produce inputs for a wide variety of models, some of which are exhibited in Fig. 1. This capability allows various approximations to be directly compared with very little effort by the user in keeping the models nominally identical.

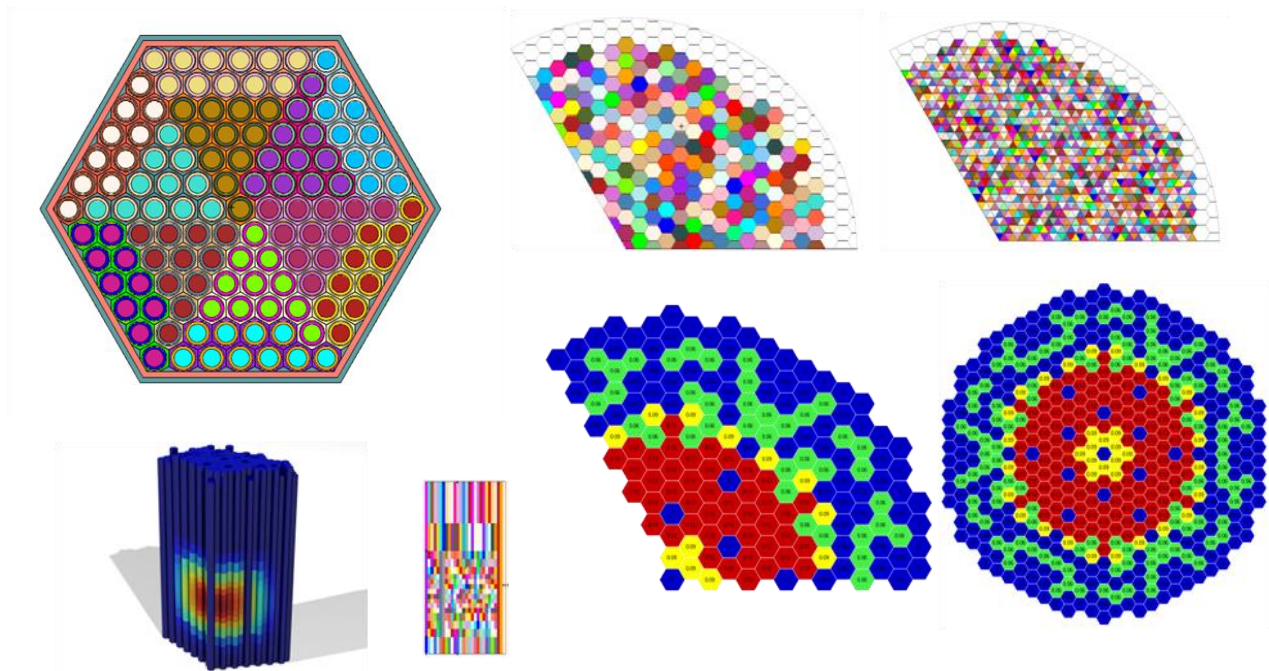


Figure 1. A collection of nominally-identical simulations automatically produced from a single GUI-based input by ARMI, including pin-detailed, homogenized hex, homogenized triangle, full-core and third-core MCNPXT, REBUS, and POVray models

2.2 Physics Implemented in ARMI

The ARMI code relies heavily on its material database, which contains temperature-dependent properties (density, thermal conductivity, heat capacity, thermal expansion, etc.) for many relevant materials extracted from the literature. Using this information, along with a nuclide-properties database of natural abundances and atomic weights (based on NIST information), all homogenization calculations are done internally. Additionally, the material-library based approach allows a designer to switch from one coolant, fuel, or structure to another without changing any code. For instance, the safety module dynamically looks up the thermal expansion coefficient of any block's current coolant material to calculate reactivity coefficients in $\text{¢}/\text{K}$. This also allows 3-D density distributions of coolant, fuel, and structure based on the thermal hydraulic calculations to be accounted for directly in the neutronics calculations.

2.2.1. Neutronics

The currently-implemented neutronics kernels in ARMI are the MC**2-2/DIF3D/REBUS-3 suite of codes and MCNPXT, a heavily modified descendent of MCNPX [7] for very high-fidelity computations (with fuel management and fuel performance coupling). Others can be added simply by writing the associated input writers and output readers. The Argonne National Laboratory (ANL) suite of codes is primarily used for day-to-day design iterations due to its high speed and is the primary kernel used in this study.

ARMI tracks the multi-group (MG) microscopic cross sections of each discrete initial enrichment in the problem with burnup dependence, regenerating them at each cycle. As initially-depleted uranium assemblies build up plutonium, their MG microscopic cross sections change substantially due to the changing neutron spectrum encountered. These changes are handled by maintaining a burnup group mesh, where a block of enrichment A that is in burnup group B gets its own set of cross sections separate from those of enrichment A, burnup group A. As a result, a large number of lattice-physics calculations must occur at each cycle. This is handled by running them in parallel, completing all required runs in less than 2 minutes/cycle. By tracking block type and burnup group on the block level, the data management is straightforward.

Besides running the main analysis loop, ARMI can also automatically produce inputs for MCNPXT from any state. These inputs can be homogenized or in pin-detail. Each axial block can have pins with different dimensions (based on user input or on thermal expansion). This feature allows code-to-code comparisons or very-high fidelity modeling without any additional modeling effort by the user (e.g. each reactor model comes with a pin-detailed MCNP model for free). Blocks without pin details (such as grid plates) are automatically detected and homogenized in the MCNP models. The fuel management from a previous ARMI run can be translated into MCNPXT move commands, allowing a full REBUS-based run with many cycles to be exactly repeated using a completely different set of solvers. Depletion is done independently for each block, which is subdivided into any number of independent burn zones, up to the number of pins in the assembly.

2.2.2. Thermal hydraulics

Several thermal-hydraulic modules have been developed within ARMI, including a basic 1-D energy balance module and a more sophisticated subchannel model with hot channel factor analysis. Additionally, ARMI automatically produces inputs for SUPERENERGY subchannel code to determine assembly peaking factors and duct temperatures. The 3-D temperature and pressure distributions from these modules are used to set the temperatures of each block, which determine the properties to be used to produce other simulation inputs. This allows coupled neutronics-thermal hydraulics as well as accurate reactivity coefficient generation. ARMI also contains a flow-orificing module that will examine the power histories of each assembly position of a core lifetime and set flow rates to keep the PCT below a user-specified limit. A restart case runs with the new flow rates to regenerate the temperature distributions. Thermal striping assessments can be done by comparing neighboring as-orificed outlet temperatures.

2.2.3 Safety and transients

ARMI automatically generates kinetics parameters and spatially-dependent reactivity coefficients at any point in a core history, including delayed neutron fraction and mean neutron lifetime. Using either perturbation theory or direct calculations on a high-performance computer, it produces fuel density, structural density, coolant density, Doppler, voided Doppler, and radial expansion coefficients. It then appends these and the corresponding power distributions, as well as assembly dimensions and other parameters to a pre-built systems code input (e.g.

SASSYS/SAS4A) which allows immediate execution and analysis of all design-basis and beyond-design basis transients.

2.2.4 Fuel performance

ARMI optionally interacts with an in-house fuel performance code. Flux, power, burnup, plutonium, and temperature histories are prepared from an initial run as input to the fuel performance codes, which return fuel height, fission gas removed, and sodium bond squeezed out vs. burnup and axial height, as well as cladding strain. In a follow-on run, ARMI updates the state of the reactor at every cycle accordingly, explicitly accounting for these effects as they occur. The fuel performance code also informs ARMI of the peak achievable burnup in each assembly based on the flux/burnup ratio, smear density, and cladding dimensions, which ARMI considers in fuel management optimization searches.

2.2.5 Core mechanical

Assemblies distort in complicated manners under irradiation and coolant pressure. The neutronics and T/H modules of ARMI provide pressure drop and dose histories to finite-element mechanical simulations and/or off-the shelf systems (e.g. NUBOW) which determines the remaining spacing between assemblies. This spacing is an important constraint in reactor design and is carefully considered in fuel management.

2.3 Use of ARMI for reactor design calculations

The automation provided by ARMI enables a philosophical shift in both exploratory and detailed reactor design. Rather than passing a design from team to team, each team constructs ARMI modules that interact with their specialized codes. Each member of each team can implement the integrated tool to obtain a full assessment of any new or perturbed design. This human parallelization enables innovation to thrive since a single person can rigorously explore their ideas without creating additional work for their teammates. It is also particularly conducive to automated multidisciplinary design optimization.

3. REFERENCE MODEL DESCRIPTION

The reference case for all studies is a pool-type sodium-cooled fast reactor (SFR) operating in a traveling wave fashion, meaning it sustains criticality given only depleted uranium without requiring further enrichment or reprocessing. Fuel management is convergent-divergent, where depleted uranium is charged in the outer ring, slowly marched inwards to a particular ring (the “jump ring”), jumped to the center, and then diverged back out to the jump ring where it is finally discharged as highly-burned fuel. All equilibrium results are taken once the core reaches an equilibrium condition given this repetitive shuffling.

Rather than making use of the fast equilibrium cycle search methodology available in REBUS, equilibrium is reached through direct cycle-by-cycle computations driven by ARMI. It has been found that the REBUS method does not give consistent results with the direct calculations for the burnup levels required by this class of reactors due to lack of fuel performance coupling and the flux-averaged microscopic cross section treatment.

The reference hex assembly design (summarized in Table I) is not expected to reach the burnup and fluence requirements of a TWR, but is adequate for understanding the modeling sensitivities and biases of interest.

Table I. Reference Core Parameters

Power	1200 MWt
Smear Density	75%
Duct thickness	3.0 mm
Clad thickness	0.45 mm
Initial slug OD	8.66 mm
Pins/assembly	169
Fuel form	U-10Zr w/ Na bond
Feed U-235 Enrichment	0.3 wt %
Structural material	HT-9
Assembly pitch	167.5 mm
Duct gap	15 mm
Wire wrap OD	1 mm
Fueled height	250 cm
Core Inventory	147 MT HM
Number of assemblies	517

The core contains 10 control rods and 3 diverse safety rods, all using natural or enriched B₄C as poison. Rods remain fully withdrawn in all cases unless otherwise noted.

4. MODELING SENSITIVITIES

By running ARMI with various mesh resolutions and physics couplings on the reference case, modeling biases were explored. The parameters of interest in of each case is compared to those from the highest-resolution case in each set of calculations with results in percent.

4.1 Neutronic and Depletion Axial Mesh Resolution

In this section, we discuss the errors made by various levels of axial mesh resolution. The neutronics mesh and the depletion mesh are varied independently; for the neutronics mesh studies, a constant depletion mesh with 10 points was maintained whereas in the depletion mesh studies, a constant neutronic mesh with 24 points was used.

4.1.1 Sensitivities due to the neutronic mesh

The neutronics code DIF3D as implemented within REBUS solves the hex-z nodal diffusion equation on the core-wide planar mesh. Nodal diffusion is well-known to be far superior to finite

difference in terms of accuracy per mesh point. Starting from one neutronic mesh point for each of the ten depletion zones and increasing to 4 neutronic mesh points per depletion zone, the results in Table II confirm that the BOL error is very low at 3.1 pcm. Propagating through depletion to the beginning-of-equilibrium cycle (BOEC) state, this grows to 25.6 pcm. As mesh points are added, k_{eff} drops, discharge burnup (BU), measured in % Fissions per heavy metal atom (% FIMA) increases slightly, the coolant temperature coefficient (CTC) is constant, and the effective delayed neutron fraction (β_{eff}) drops very slightly. All cases in the table are compared to the highest-fidelity case (4 neutronics points per depletion mesh).

Table II. Sensitivity of equilibrium parameters to the neutronic mesh

Neutronics Mesh Points per Depletion Mesh	1 point	2 points	3 points	4 points
Mesh Height (cm)	22.32	11.16	7.44	5.58
BOL k_{eff} (pcm from ref.)	3.1	0.6	<0.1	0.00%
BOEC k_{eff} (pcm from ref.)	25.6	6.8	<0.1	0.00%
BOEC APD (MW/m²)	-0.17%	-0.02%	0.00%	0.00%
BOEC BU (% FIMA)	-0.60%	-0.10%	0.00%	0.00%
BOEC CTC (¢/K)	-0.01%	0.00%	0.00%	0.00%
BOEC β_{eff}	0.04%	0.01%	0.00%	0.00%

In Table II and others, EQ APD refers to the peak equilibrium cycle Areal Power Density, defined as the maximum assembly power divided by the core area occupied by an assembly. It is a useful figure of merit since it is proportional to the coolant temperature rise in the assembly, and is therefore closely related to peak cladding temperature. It is also known as the axially-integrated power density.

4.1.2 Sensitivities due to the depletion mesh

The parameters of interest are much more sensitive to variations in the depletion mesh than to those in the neutronic mesh, as seen in Table III. Errors from averaging the depletion over large zones lead to errors of hundreds of pcm in the very coarse mesh. Errors in areal power density and in peak discharge burnup are accounted for by the nodal method with inter-node peaking factors, and therefore the values reported in table are overstatement of the error inherent in the DIF3D/REBUS method, but for implementations of data management systems such as ARMI, these large differences in average values should be well understood and carefully tracked. The errors in the CTC and the delayed neutron fraction are less than 1%.

Table III. Sensitivity of equilibrium parameters to the depletion mesh

Total Depletion Mesh Points	1 point	2 points	4 points	8 points	16 points
Mesh Height (cm)	178.57	89.29	44.64	22.32	11.16
BOEC k_{eff} (pcm from ref.)	624.9	567.1	152.5	72.2	0.00
BOEC APD (MW/m²)	-2.39%	-2.19%	-1.75%	-0.30%	0.00%
BOEC BU (% FIMA)	-22.23%	-21.77%	-6.04%	-1.06%	0.00%
BOEC CTC (¢/K)	-0.90%	-0.91%	0.38%	0.42%	0.00%
BOEC β_{eff}	0.56%	0.54%	0.13%	0.02%	0.00%

4.2 The Degree of Spatial Homogenization

To compare pin-detailed cases with homogenized cases, the MCNPXT kernel of ARMI was required rather than the homogenized-only DIF3D/REBUS kernel. Nominally identical models were created with homogenized hexagons and pin-detailed assemblies with both 1 and 6 burn zones per block. Fuel management was identical to that of all other reference cases in this study, driven by the move commands available in MCNPXT. In the pin-detail model, the wire wrap was homogenized into the coolant. In all cases, independent cells and materials had to be specified in the MCNP input, giving the largest inputs automatically produced by ARMI more than 80k cells and universes and 75k materials, for a total of over 800k lines. Cases of this size were run efficiently on 240 processors on a high performance computer thanks to the very much work that has gone into the development of MCNPXT. Again, these extremely large inputs are produced and executed at the click of a button thanks to the power of ARMI.

Homogenization results are shown in Table IV. The pin detail case had less reactivity than the homogenized case, both at BOL and at equilibrium. Typically, spatial self-shielding gives a reactivity bonus to the heterogeneous case, but in this case, differences in the spectrum overpower this effect. The homogenized case has 1.5% higher fast flux fraction (>0.1 MeV). Details of these effects are being studied.

Table IV. Sensitivity of equilibrium parameters to the homogenization approximations with one burn zone per hex block

Mesh	Homogeneous	Pin Detail	Difference
BOL k_{eff}	1.0733 ± 0.00017	1.0688 ± 0.00016	450 ± 23 pcm
BOEC k_{eff}	1.03520 ± 0.00134	1.02364 ± 0.00137	1156 ± 192 pcm
EQ APD (MW/m²)	313.7	314.0	-0.1%
EQ BU (% FIMA)	37.5	38.1	1.57%

4.3 Explicit Fuel Performance

As metallic fuel is irradiated, fission gas pressure causes it to grow quickly until it contacts the clad at low burnup (typically within <2% FIMA). The fuel remains in soft contact with the cladding until low-density fission products build up enough to cause hard contact and eventually strain the cladding to its limit. Typically, metallic fuel is fabricated with a low smear density, where the fuel pin initially takes up a fraction (such as 75%) of the space within the cladding. The large gap is typically filled with sodium to allow heat transfer out of the pin. As the fuel expands with burnup, the sodium bond gets squeezed out of the active core and into the plenum. Meanwhile, as the fuel becomes porous, some of the pores interconnect and fission gas can be released. Many of the upper peak fission products beta-decay into xenon and are released from the fuel. The reactivity effects of fuel expansion and its associated bond squeeze-out and fission gas release are large and must be modeled dynamically to understand the evolution of true reactor operation. These reactivity effects are shown in Table V.

An additional effect of fuel axial expansion is that it raises the axial positions of both the burnup and flux distributions as fuel is burned. As a result, incoming fresh fuel (still at its original length) is irradiated at an above-center level by burned fuel that has grown axially. This causes the equilibrium burnup distribution becomes shifted upward. In the example model, the peak burnup location shifts upward by 7 cm, from a core-center location to one slightly above it (125 cm to 133 cm from the bottom of the fuel column). The burnup distribution is kept from moving up further by the increase in leakage out the top of the fueled region. This effect was measured using the MCNPXT physics kernel, because of its ability to easily accept varying axial zone sizes. ARMI can also be used to model this situation in REBUS by re-homogenizing the axially-expanding fuel zones (tracked in ARMI) into a fixed REBUS spatial mesh.

Table V. Sensitivity of equilibrium parameters to coupled fuel performance

Fuel Performance	None	Axial Expansion	F.G. Removal	Bond Removal	All
BOEC k_{eff} (pcm from ref.)	392	-1144	858	738	0
BOEC APD (MW/m²)	-2.73%	-0.86%	-1.33%	-0.71%	0.00%
BOEC BU (% FIMA)	2.76%	1.72%	-1.34%	0.81%	0.00%
BOEC CTC (¢/K)	-5.99%	6.26%	-11.07%	-1.40%	0.00%
BOEC β_{eff}	0.06%	-0.59%	0.61%	0.04%	0.00%

4.4 Thermal Hydraulic Feedback

The fuel, coolant, and structural densities are typically assumed at some core-average temperature. However, the temperature gradients can be substantial. The effects on a high-burnup system with regard to T/H feedback are discussed in this section. To couple the neutronics and T/H, an operator splitting method is used, where the neutronics simulation produces a power distribution, which the T/H module turns into a temperature distribution. Then, in a second iteration, the neutronics code uses newly thermally-expanded dimensions and densities to produce an updated power distribution. The number of these physics iterations is a user input to ARMI. The results shown in Table VI indicate that the effect of this coupling is on the order of 50 pcm in terms of equilibrium reactivity, and below 1% for other parameters of interest, with the overall power peaking factor as the exception with a 1.5% difference.

Table VI. Sensitivity of equilibrium parameters to coupled T/H

Coupling iterations	0 iterations	1 iteration	2 iterations
BOEC k_{eff} (pcm from ref.)	-51	7	0
BOEC APD (MW/m²)	0.06%	-0.01%	0.00%
BOEC BU (% FIMA)	0.16%	0.00%	0.00%
BOEC CTC (¢/K)	0.00%	1.17%	0.00%
BOEC β_{eff}	0.00%	-0.03%	0.00%
BOEC F_q	-1.49%	0.00%	0.00%

4.5 Burnup Dependent Cross Sections and Fission Products

Deterministic fast reactor calculations typically assume constant microscopic cross sections and fission product distributions in lumped fission products. This stationary approximation breaks down as neutron spectrum shifts with changing fuel composition at high burnup. Additionally, as fission products build up, they begin to influence the spectrum. To account for the changes in the fuel composition as a function of burnup, the microscopic cross sections are continually regenerated by MC² for a representative assembly in each burnup group range. For this study, four burnup groups were used for each representative assembly type.

The reference solution was created by generating a new cross-section library for each cycle using the beginning-of-cycle representative compositions within each burn group. After eventually reaching equilibrium, the complete cross-section library was used to determine the effects of omitting particular burnup groups. The now-fixed cross sections within each burn group are used to again model the reactor from startup to equilibrium. The effect of omitting different burnup groups can be seen in Table VII.

Additionally, a detailed fission product model has been developed that uses burnup dependent fission product yields for the parent nuclides U-235, U-238, Pu-239, Pu-240, and Pu-241. These burnup dependent yields were generated using the SCALE[9] code from Oak Ridge National Laboratory. A TRITON model of representative assemblies generated high burnup binary libraries that were then used in ORIGEN calculations using modified binary libraries to focus on single nuclides with time-dependent fluxes to preserve interaction rates. The net result of this approach gives an approximation of the fission product composition from a parent nuclide that includes fission product transmutation over time. These nuclide compositions were then used to adjust the spectrum calculation that produces the collapsed cross-section sets used for the simulation. The effects of this process are shown in Table VII in the Detailed FP column.

Table VII. Modeling effect of using burnup-dependent microscopic cross sections

	1 group [1]	2 groups [2]	3 groups [3]	4 groups [4]	Detailed FP
BOEC (pcm from ref.)	-1029	-71	-26	-11	262
BOEC APD (MW/m²)	0.58%	0.16%	0.05%	0.00%	-0.18%
BOEC BU (% FIMA)	0.00%	0.06%	0.03%	0.00%	0.92%
BOEC CTC (¢/K)	0.00%	1.35%	0.00%	0.45%	0.00%
BOEC β_{eff}	0.76%	0.01%	0.01%	0.00%	0.00%

[1] Burnup range from 0-3%

[2] Burnup range from 0-3% and 3-10%

[3] Burnup range from 0-3%, 3-10%, and 10-20%

[4] Burnup range from 0-3%, 3-10%, 10-20%, 20-100%

When using only the BOL cross-section set, the calculation under predicts equilibrium reactivity by 1029 pcm from the reference solution. When using the two group cross-section set, the calculation bias is reduced to 71 pcm. The effects of adding additional groups of cross sections into the model clearly converge to the reference solution at an equilibrium cycle. Due to enforcing a constant power normalization, the treatment of the cross-sections does not have a large effect on the equilibrium areal power density or burnup. It is also worth noting that the detailed fission product model shows an increase in reactivity by 262 pcm. This change is attributed to the fact that as fission products absorb neutrons, their absorption cross-sections will also change. In high burnup fuel, the accumulated effect of the depletion of the highly absorbing fission products will have an impact on the reactivity of the system.

While there may be a clever selection of single or few-group burnup bounds that solve a particular fast reactor problem well, care should be taken when modeling the transition to high burnup to maintain accuracy over the entire simulation.

4.6 Explicit Control Rod Insertion

To determine the effect of dynamically modeling control rod insertion, the uncontrolled reference model is compared to a case with a critical control rod search at each cycle out to equilibrium. In the uncontrolled case, the reactor is modeled with the control rods fully withdrawn during the entire life of the reactor core. Conversely, non-depleting B4C control rods are inserted as an entire bank in ~19.5 cm increments until the reactor is just critical for the controlled case. This coarse control does not perfectly produce a critical reactor and in this case the BOEC k_{eff} was 1.003. The control rod iteration is run by ARMI in parallel, requiring 1-2 extra computational minutes per cycle. This process is repeated at the beginning of every cycle for the entire reactor life using the exact same fuel management plan as the uncontrolled case. The net effect of explicit control rod modeling on the equilibrium burnup distribution is shown in Figure 2.

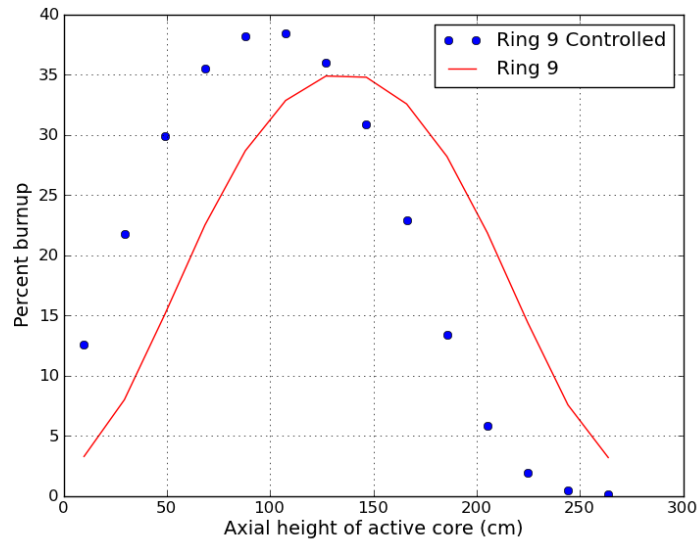


Figure 2. Percent burnup in radial ring 9 vs. axial height in controlled and uncontrolled equilibrium case

The uncontrolled equilibrium burnup distribution appears as a cosine function with the burnup centroid located at 136 cm above the grid plate. The controlled case looks substantially different with a non-uniform burnup distribution and a burnup centroid moves down 34 cm. As summarized in Table VIII., besides changing the location of the power distribution in the reactor, the controlled equilibrium case requires additional peak burnup of the fuel. In this particular comparison, the uncontrolled case has a peak burnup of 35.3% FIMA while the controlled peak burnup is 38.8% FIMA. This significant difference between the two models demonstrates that explicit control rod modeling must be considered for accurate simulation of fuel and neutronic performance, especially for cases with large excess reactivity.

Table VIII. Modeling effect of critical control rods at BOEC

Case	Reference	Controlled*	Difference
BOEC k_{eff}	1.013812	1.006463	-725 (pcm)
BOEC APD (MW/m²)	308.50	318.31	3.18%
BOEC BU (% FIMA)	35.3	38.8	-9.92%
BOEC CTC (ϕ/K)	0.223	0.220	1.35%
BOEC β_{eff}	0.003397	0.003380	0.50%
BOEC Burnup Centroid	136.1	101.8	-25.2%

*The uncontrolled k_{eff} is shown for the controlled case

4.7 Burn Chain Truncation

In standard quasi-static microscopic depletion calculations, the actinide chains are modeled with various truncations. Minor actinides build up and significantly in high burnup fuels, and calculations are increasingly sensitive to their treatment. While a calculation that tracks every minor actinide can be considered the most accurate approach, the additional size of the transmutation matrices adds additional computational and memory requirements. To speed up the computation time, some of the minor actinides can be excluded from the calculation if their overall effect is low on the simulation. To investigate the minimum number of actinides required to model a high-burnup reactor, the burn chain was truncated at various nuclides. Anything in a transmutation chain that would be larger than the specified isotope is transmuted into a non-interacting dummy nuclide. The effect of this truncation can be seen in Table IX.

Table IX. Modeling effect of burn chain truncation

Actinide Range	Pu-240*	Pu-242*	Cf-252*
BOEC k_{eff} (pcm from ref.)	-891	-26	0
BOEC APD (MW/m²)	1.21%	0.20%	0.00%
BOEC BU (% FIMA)	-1.79%	-0.08%	0.00%
BOEC CTC (ϕ/K)	3.59%	0.00%	0.00%
BOEC β_{eff}	-0.67%	0.16%	0.01%

*Reference solution contains actinides up to Cm-247

There is little difference between the different burn chain truncations after including all plutonium isotopes up to Pu-242. However, there is a significant effect on the calculation if the burn chain is truncated at Pu-240. The fuel burnup decreases while the maximum areal power density increases. The higher areal power result stems from the fact that Pu-241 and Pu-242 isotopes build up with higher burnup and are in their highest concentrations around the jump ring before they are discharged. This effect spreads the power out over a larger area of the core, reducing the peaking effect in the reference case. The lower burnup seen in the Pu-240 truncated burn chain comes from the redistribution of flux axially at the center of the core. This spreads out the power producing region axially over the central assemblies that are quickly breeding up Pu-239 and Pu-240. For fuel cycle calculations, truncating the burn chain at Cm-247 appears to be sufficient approximation for most problems. Related work found that modeling up to Cf-252 [8] is important in other regards, such as in the radiological source term.

5. CONCLUSIONS

The newly-developed ARMI code has been successfully implemented to quantify the modeling biases at equilibrium that result from many common simulation approximations. The abstract model provided by ARMI allows a build-once, run-many approach to the analysis of multiphysics core phenomena.

For a large SFR core, it was confirmed that a coarse neutronic and depletion axial mesh on the order of 20 cm is sufficient for most fuel cycle modeling at equilibrium. From this point, doubling the resolution of the depletion mesh reduces the equilibrium k_{eff} by ~ 70 pcm, whereas doubling the neutronics mesh results in a negligible reduction. It was demonstrated that coupled fuel performance is essential to model high-burnup reactors, with the neglect of axial expansion alone producing a 1000 pcm over-prediction of the equilibrium k_{eff} . Modeling these coupled effects requires sophisticated data management capabilities. Thermal hydraulic feedback in steady state for a sodium coolant was shown to have marginally negligible reactivity effects at equilibrium (a 51 pcm under-prediction without it). A burnup dependent microscopic cross section model is essential, but having only two groups recovers most of the bias. Explicit modeling of critical control rod positions is extremely necessary, with very high sensitivities seen in burnup distributions and reactivity. Finally, it was confirmed that truncating the burn chain at Cm-247 is a valid approximation even for high burnup reactors, at least for fuel cycle calculations.

A large amount of analysis was done systematically by a small team using the ARMI. This system can increase innovation turnaround and reduce design times while reducing human error. As more modules are developed and automated, ARMI continues to become more conducive to automated multidisciplinary design optimization, and development towards this goal is ongoing.

ACKNOWLEDGEMENTS

Many thanks to Chuck Whitmer and George Zimmerman for their enhancements that make up MCNPXT enabling the extreme fidelity cases, to the current and past contributors to ARMI, and to all the developers of all the other codes that have so far provided the kernels for ARMI.

REFERENCES

1. J. Gilleland, C. Ahlfeld, et. al, “Novel Reactor Designs to Burn Non-Fissile Fuels,” *Proc. of ICAPP*, Anaheim CA, June 8-12, (2008).
2. N. Touran, P. Hejzlar, S. Mazurkiewicz, R. Petroski, J. Walter, C. Whitmer, “Technical Considerations and Capabilities of a Near-Term Deployable Traveling Wave Reactor Core,” *Trans. Am. Nucl. Soc.*, Hollywood, FL, June 26-30, Vol. 104, pp. 934-936 (2011).
3. G. Aliberti, G. Palmiotti, M. Salvatores, T.K. Kim, T.A. Taiwo, M. Anitescu, I. Kodeli, E. Sartori, J.C. Bosq, J. Tommasi, “Nuclear Data Sensitivity, Uncertainty, and Target Accuracy Assessment for Future Nuclear Systems,” *Ann. Nucl. Energy*, **33**, pp.700-733 (2006).
4. G. van Rossum, et al. “Python Programming Language,” <http://www.python.org> (2011).
5. B. Toppel, A. Rago, D. O’Shea, “MC2: A Code to Calculate Multigroup Cross Sections,” ANL-7318, Argonne National Laboratory (1967).
6. A. P. Olson, “A Users Guide for the REBUS-PC code, Version 1.4.” ANL/RERTR/TM-32, Argonne National Laboratory (2002).
7. J. Hendricks, G. Mckinney, M. Fensin, M. James, R. Johns, J. Durkee, J. Finch, D. Pelowitz, L. Waters, and F. Gallmeier, “MCNPX, Version 26E”, LAUR-07-6632, Los Alamos National Laboratory (2007).
8. S. Bays, S. Piet, M. Pope, G. Youinou, A. Dumontier, D. Hawn, “Transmutation Dynamics: Impacts of Multi-Recycling on Fuel Cycle Performances,” INL/EXT-09-16857, Idaho National Laboratory (2009).
9. SCALE: *A Modular Code System for Performing Standardized Computer Analyses for Licensing Evaluation*, ORNL/TM-2005/39, Version 6, Vols. I-III, Oak Ridge National Laboratory, Oak Ridge, Tennessee, January 2009. Available from Radiation Safety information Computational Center at Oak Ridge National Laboratory as CCC-750